

Inferences for Random Graphs Evolved by Clustering Attachment

Natalia Markovich · Maksim Ryzhov · Marijus Vaičiulis

Received: date / Accepted: date

Abstract The evolution of random undirected graphs by the clustering attachment (CA) both without node and edge deletion and with uniform node or edge deletion is investigated. Theoretical results are obtained for the CA without node and edge deletion when a newly appended node is connected to two existing nodes of the graph at each evolution step. Theoretical results concern to (1) the sequence of increments of the consecutive mean clustering coefficients tends to zero; (2) the sequences of node degrees and triangle counts of any fixed node which are proved to be submartingales. These results were obtained for any initial graph. The simulation study is provided for the CA with uniform node or edge deletion and without any deletion. It is shown that (1) the CA leads to light-tailed distributed node degrees and triangle counts; (2) the average clustering coefficient tends to a constant over time; (3) the mean node degree and the mean triangle count increase over time with the rate depending on the parameters of the CA. The exposition is accompanied by a real data study.

Keywords Random graph · Evolution · Clustering attachment · Attachment probability · Clustering coefficient · Extreme value index

N. Markovich
V.A.Trapeznikov Institute of Control Sciences, Russian Academy of Sciences
Tel.: +7(495)3348820
E-mail: nat.markovich@gmail.com

M. Ryzhov
V.A.Trapeznikov Institute of Control Sciences, Russian Academy of Sciences
Tel.: +7(495)3348820
E-mail: ryzhov@phystech.edu

M. Vaičiulis
Vilnius University, Institute of Data Science and Digital Technologies
Akademijos st. 4, LT-08663 Vilnius, Lithuania
E-mail: marijus.vaiciulis@mif.vu.lt

1 Introduction

Network evolution attracts interest of researchers due to numerous applications (Avrachenkov & Dreveton, 2022; Ghoshal et al., 2013; van der Hofstad, 2017; Norros & Reittu, 2006; Wan et al., 2020). The popular mechanism to model growing real-world networks and to explain a power-law distribution of their node degrees is a linear preferential attachment (LPA). It is applied both to directed and undirected graphs, see Norros and Reittu (2006), Wan et al., (2020) among others. The attachment of new nodes starts from an initial network. A newly appended node may connect to $m_0 \geq 1$ existing nodes. By the LPA a newly appended node chooses an existing node i randomly in the graph $G = (V, E)$ (V and E denote sets of nodes and edges) with a probability proportional to its degree k_i (i.e. the number of edges of node i): $P_{PA}(i) = k_i / \sum_{j \in V} k_j$ (Bagrow & Brockmann, 2012). The LPA models provide a "rich-get-richer" mechanism since the earliest appended nodes get likely more edges. This leads to a power-law node degree distribution with tail index $\beta > 0$ and a constant $C > 0$:

$$P\{k_i = j\} \sim Cj^{-1-\beta}, \quad j \rightarrow \infty.$$

Here, $a_n \sim b_n$ means that the sequences a_n and b_n are asymptotically equal, i.e., $a_n/b_n \rightarrow 1$, $n \rightarrow \infty$. The distribution tail becomes heavier for a smaller β .

However, some real world networks under the constraints of geographical conditions or topological characteristics have exponential degree distribution, such as the North American Power Grid Network (Albert & Barabási, 2002), the Worldwide Marine Transportation Network (Guimerá et al., 2003) and some email networks (Deng, 2009).

In the following we focus at the clustering attachment (CA) proposed in Bagrow and Brockmann (2012) that constitutes another approach to model the evolving networks. The CA has not received a further development since it seems to be applicable to local networks corresponding to a close geolocation of nodes. The CA cannot model the evolution in real-world networks where rare giant nodes may rapidly grow. Instead of giant nodes dense communities are generated around new nodes since nodes are drawn not towards hubs, but towards densely connected groups (Bagrow & Brockmann, 2012). Transport networks may be mentioned as one of practical potential application of the CA. Really, the appearance of a new metro station in a megapolis gives rise to a rapid development of the district and generates a dense transport hub and infrastructure around. Over time, the district reaches a stable state and does not develop so fast anymore. Our paper is devoted to study the CA including the investigation of the impact of node and edge deletion which is a novelty.

The CA model can be described by a graph sequence G_t , $t = 0, 1, \dots$. Let us denote the set of nodes and edges in the graph $G_t = (V_t, E_t)$ at step t , $t \geq 0$ as V_t and E_t , respectively, and their cardinality as $\|V_t\|$ and $\|E_t\|$. The evolution starts with a finite undirected initial graph G_0 which consists

of $\|V_0\| \geq 1$ nodes and $\|E_0\| \geq 0$ edges. We form G_{t+1} from G_t for $t \geq 0$ by the following rules:

(i) We append a new node $\|V_0\| + t + 1$ to G_t .

(ii) By using a weighted sampling without replacement (see, e.g. Devroye (1986)) we choose a set of nodes $W_t \subset V_t$, such that $\|W_t\| = m_0 \geq 2$, and create m_0 new edges between a newly appended node $\|V_0\| + t + 1$ and m_0 selected nodes. The probabilities

$$P_{CA}(i, t) = \frac{c_{i,t}^\alpha + \epsilon}{\sum_{j \in V_t} c_{j,t}^\alpha + \|V_t\| \epsilon}, \quad i \in V_t, \alpha > 0 \quad (1)$$

and

$$P_{CA}(i, t) = \frac{\mathbf{1}\{c_{i,t} > 0\} + \epsilon}{\sum_{j \in V_t} \mathbf{1}\{c_{j,t} > 0\} + \|V_t\| \epsilon}, \quad i \in V_t, \alpha = 0 \quad (2)$$

are used as the weights for the sampling without replacement. Here, $\mathbf{1}\{\cdot\}$ denotes the indicator of the set $\{\cdot\}$ and $\alpha, \epsilon \geq 0$ are attachment parameters. The clustering coefficient $c_{i,t}$ of node $i \in V_t$ is defined by

$$c_{i,t} = \begin{cases} 0, & k_{i,t} = 0 \text{ or } k_{i,t} = 1, \\ 2\Delta_{i,t} / (k_{i,t}(k_{i,t} - 1)), & k_{i,t} \geq 2. \end{cases} \quad (3)$$

Here, $\Delta_{i,t}$ is the number of links between neighbors of node i or, equivalently, the number of triangles involving node i , and $k_{i,t}$ denotes the degree of node i , both at time t . Hereinafter, where it is needed, we will use notation $CA^{(\alpha, \epsilon)}$.

Assumptions on the initial graph G_0 depend on ϵ . If $\epsilon > 0$ it is enough to assume that $\|V_0\| \geq m_0$. If $\epsilon = 0$, then we have to assume that $\|\tilde{V}_0\| \geq m_0$, where the sequence of sets $\tilde{V}_0, \tilde{V}_1, \dots$ is defined as follows: $\tilde{V}_n = \{i \in V_n : c_{i,n} > 0\}$, $n \geq 1$. Let \tilde{E}_t denote the set of all possible edges between pairs of nodes $\{i_1, i_2\}$, such that $i_1 \in \tilde{V}_t, i_2 \in \tilde{V}_t, i_1 \neq i_2$, including probably not existing edges. It is worth noting that $(\tilde{V}_n, \tilde{E}_n)$ is a complete graph.

A probability mass function $P_{CA}(i, t)$, $i \in V_t$ for the limit case $\alpha \downarrow 0$ is constructed by us keeping in mind the relation $x^\alpha \rightarrow 1$ as $\alpha \downarrow 0$ for any fixed positive x and by the convention $0^0 = 0$.

The CA model with probabilities

$$P_{CA}(i, t) \propto c_{i,t}^\alpha + \epsilon \quad (4)$$

was used in Bagrow and Brockmann (2012). We recall that $x \propto y$ means that there is a non-zero constant C such that $x = C \cdot y$. In fact, (1) and (4) define the same conditional probabilities with $C = M_t$, where

$$M_t = \left(\sum_{j \in V_t} c_{j,t}^\alpha + \|V_t\| \epsilon \right)^{-1}.$$

Such kind of the CA excludes the appearance of multiple edges. Furthermore, the sets V_t and E_t grow linearly in t : $\|V_t\| = \|V_0\| + t$ and $\|E_t\| = \|E_0\| + m_0 t$,

$t \geq 0$ without the node and edge deletion. Whence it immediately follows that the ratio $\|E_t\|/\|V_t\|$ tends to m_0 as $t \rightarrow \infty$.

In the paper we consider several modifications of the CA. One of them allows a node deletion when a new node is appended. Specifically, together with (i), (ii), one more rule is added:

(iii) We choose one node from the set V_t uniformly, i.e. each node with probability $1/\|V_t\|$, and delete it. We remove also all edges belonging to this node.

The second modification of the CA model concerns the allowance of an edge deletion when a new node is appended. Then the rule (iii) is replaced by the following:

(iv) We choose one edge from the set E_t uniformly, i.e. each edge with probability $1/\|E_t\|$, and delete it.

Further, we keep the notation CA for the clustering attachment model generated by rules (i), (ii).

In contrast to the PA, the intuition outlined in Bagrow and Brockmann (2012) shows that the CA does not lead to a power-law node degree distribution, but to an exponential light-tailed distribution. Our **first objective** is to find lower and upper bounds for the increment of consecutive mean clustering coefficients over time; to derive that (total) node triangle counts and node degrees are submartingales irrespective of the CA parameters α and ϵ in (1), (2). In Markovich and Vaičiulis (2024) a special attention was devoted to the model $CA^{(0,0)}$. It was proved there without additional assumptions that a total triangle count tends to infinity almost surely for the latter model.

Our **second objective** is to check the hypothesis of a light-tailed node degree distribution with regard to α , ϵ in (1) as well as to evolution strategies, namely, without node and edge deletion and with the deletion of one of the existing nodes or edges each time when a new node is appended. This is done by the extreme value index (EVI) estimation of the node degree, see Section 2.2 for the EVI definition. The EVI allows us to distinguish between light- and heavy-tailed distributions. For heavy-tailed distributions, the value of the EVI indicates the heaviness of the distribution tail. The EVI will be estimated by several known semi-parametric estimators. Moreover, our simulation study aims to confirm the results obtained in the propositions.

The paper is organized as follows. Related definitions and results are given in Sect. 2. Theoretical results are provided in Sect. 3. The simulation study is presented in Sect. 4. Sect. 5 illustrates our theoretical results for real networks. We finalize with the conclusions in Sect. 6.

2 Related definitions and results

2.1 Mean clustering coefficient

The clustering coefficient $c_{i,t}$ of node $i \in V_t$ in (3) measures its tendency to form triangles of the nearest nodes in its neighborhood. The average clustering

coefficient for an undirected graph $G_t = (V_t, E_t)$, $t \geq 0$ is defined by

$$\bar{C}_t = \frac{1}{\|V_t\|} \sum_{i \in V_t} c_{i,t}. \quad (5)$$

For the CA model the definition (5) can be rewritten as follows:

$$\bar{C}_t = \frac{1}{\|V_0\| + t} \sum_{i=1}^{\|V_0\|+t} c_{i,t}.$$

The statistic \bar{C}_t may be used to distinguish between geometric and non-geometric networks. We refer to Bringmann et al. (2019); Michielan et al. (2022) for the explanation of the last two notions. Roughly speaking, in geometric networks each node is positioned in a geometric space and there is a distance to other nodes that can be measured. Typically, if the value of \bar{C}_t does not vanish in t , then this is considered to be evidence for a geometry. For example, the average clustering coefficient of a geometric inhomogeneous random graph does not vanish as t increases (Bringmann et al., 2019). For hyperbolic random graphs, \bar{C}_t converges in probability to a positive constant (Fountoulakis et al., 2021). For the inhomogeneous random graphs the decay of \bar{C}_t can be extremely slow (Michielan et al., 2022).

2.2 Extreme value index

Let us recall the definition of the EVI (de Haan & Ferreira, 2007). A quantile type function U associated with an arbitrary cumulative distribution function (cdf) $F(x)$ is defined by

$$U(t) = \begin{cases} 0, & 0 < t \leq 1, \\ \inf \{x : F(x) \geq 1 - (1/t)\}, & t > 1. \end{cases}$$

The function $U(t)$ is said to be of an extended regular variation if there exists a positive function $a(t)$ such that for some $\gamma \in \mathbb{R}$ and all $x > 0$, it holds

$$\lim_{t \rightarrow \infty} \frac{U(tx) - U(t)}{a(t)} = \begin{cases} \ln(x), & \gamma = 0, \\ (x^\gamma - 1)/\gamma, & \gamma \neq 0. \end{cases}$$

The parameter γ is called the EVI. If $\gamma > 0$ holds, then the EVI and tail index β are related by $\beta = 1/\gamma$. For example, EVI of Burr or Fréchet distribution is positive. The examples of light-tailed distributions with $\gamma = 0$ are an exponential distribution and a normal distribution, while the examples of light-tailed distributions with $\gamma < 0$ are uniform and beta distributions. It is worth mentioning that not all distributions belong to the class of extended regular variation. A Poisson distribution can be taken as an example.

3 Main Results

In this section we provide our theoretical results related to the CA model. The model is considered without node and edge deletion here.

3.1 Weighted sampling without replacement

Let us adopt the sampling procedure for our purposes. Suppose that a random graph $G_t = (V_t, E_t)$ is generated after t evolution steps. We denote the unordered pair of nodes chosen from V_t by using weighted sampling without replacement (WSwR) as W_t . Let a set \mathcal{E}_t be such, that (V_t, \mathcal{E}_t) forms a complete graph. The attachment probabilities

$$P(W_t = \{i_1, i_2\}), \quad \{i_1, i_2\} \in \mathcal{E}_t$$

are needed to generate the $CA^{(\alpha, \epsilon)}$ model.

Proposition 1 *Let the sequence of random graphs G_1, G_2, \dots be generated by the $CA^{(\alpha, \epsilon)}$ model with the initial graph G_0 and parameters $\alpha > 0$, $\epsilon \geq 0$ and $m_0 = 2$. Then for any $\{i, j\} \in \mathcal{E}_t$,*

$$P(W_t = \{i, j\}) = \frac{P_{CA}(i, t)P_{CA}(j, t)(2 - P_{CA}(i, t) - P_{CA}(j, t))}{(1 - P_{CA}(i, t))(1 - P_{CA}(j, t))}. \quad (6)$$

Corollary 1 *Depending on $\epsilon > 0$ or $\epsilon = 0$ the collection of conditional probabilities (6) form a conditional probability distribution on \mathcal{E}_t and $\tilde{\mathcal{E}}_t$, respectively.*

3.2 Bounds for increments of the mean clustering coefficients

We investigate the following sequences of a fixed node $i \in V_t$. Namely, we consider node degrees $\{k_{i,t}\}$, the triangle counts $\{\Delta_{i,t}\}$ and the clustering coefficients $\{c_{i,t}\}$ for all $t \geq 0$. For any $t \geq 1$ we assume

$$k_{\|V_0\|+t,s} = 0, \quad 0 \leq s < t. \quad (7)$$

The same assumption holds for the rest of the sequences. Note that the sequence $\{k_{i,t}\}_{t \geq 0}$ is non-decreasing, i.e., $k_{i,t} \leq k_{i,t+1}$ for any $t \geq 0$. The same is valid for $\{\Delta_{i,t}\}_{t \geq 0}$. As for $\{c_{i,t}\}_{t \geq 0}$, it is stated in Bagrow and Brockmann (2012) that "even when a new triangle is formed, the clustering coefficient after an attachment is almost always less than it was before". Here, the notion "almost always" is used in the sense that it might be $c_{i,t} > c_{i,t+1}$ for some $t \geq 0$. Let us consider the following counter examples.

Example 1 Let $V_0 = \{1, 2, 3, 4\}$ hold and the graph G_0 be a rectangle. Let the numbering of nodes go clockwise. Assuming $m_0 = 2$, a newly appended node is connected with nodes 1 and 3 at each time step $t \rightarrow t+1$, $t \geq 0$. Under such evolution we have $\Delta_{i,t} = 0$ and consequently, $c_{i,t} = 0$ for any $i \in V_t$ and $t \geq 0$.

The next simple modification of the initial graph G_0 demonstrates that the clustering coefficients of some nodes can remain constant.

Example 2 Let G_0 be the same rectangle as in the previous example but with diagonal connecting nodes 1 and 3. Under the same evolution as in the previous example, we have $c_{2,t} = c_{4,t} = 1$ for all $t \geq 0$ by (3).

The last two examples demonstrate the impact of the initial graph G_0 on the average clustering coefficient \bar{C}_t , see (5) for its definition. Turning back to Example 1 we have $\bar{C}_t = 0$ for any $t \geq 0$. In Example 2 we have by

$$c_{1,t} = c_{3,t} = \frac{2}{t+3}, \quad c_{2,t} = c_{4,t} = 1$$

and $c_{i,t} = 1$ for $t \geq 1$, $\|V_0\| < i \leq \|V_0\| + t$, where $\|V_0\| = 4$, that $\bar{C}_t = 4/((t+3)(t+4)) + (t+2)/(t+4)$ holds. Whence it follows $\bar{C}_t \rightarrow 1$ as $t \rightarrow \infty$.

Let us consider the behaviour of $\bar{C}_t - \bar{C}_{t+1}$ in a general case.

Proposition 2 *Let $G_t = (V_t, E_t)$, $t \geq 0$ be the sequence of the CA evolved graphs. Assume that the evolution parameter m_0 satisfies $m_0 = 2$. Then for any $t \geq 0$, it holds*

$$-\frac{3}{\|V_0\| + t + 1} \leq \bar{C}_t - \bar{C}_{t+1} \leq \frac{7/3}{\|V_0\| + t + 1}. \quad (8)$$

We have several notices related to Prop. 2.

- Remark 1*
1. Proposition 2 can be generalized to the case $m_0 \geq 2$.
 2. The inequality (8) is true for any realization of the $CA^{(\alpha, \varepsilon)}$ model. Since we do not use distribution (1) in our proof, (8) holds true if we replace the CA model by the LPA model.
 3. Let $0 \leq t < t'$ hold. By using the inequality $|\bar{C}_{t'} - \bar{C}_t| \leq \sum_{s=t}^{t'-1} |\bar{C}_{s+1} - \bar{C}_s|$ and (8) it follows that

$$|\bar{C}_{t'} - \bar{C}_t| \leq \sum_{s=t}^{t'-1} \frac{3}{\|V_0\| + s + 1} \leq 3(H(t') - H(t)),$$

where $H(t) = \sum_{s=1}^{t-1} 1/s$.

By using the inequalities $\ln(t-1) \leq H(t) \leq 1 + \ln(t-1)$, $t \geq 2$ we get

$$|\bar{C}_{t'} - \bar{C}_t| \leq 3 \ln \left(\frac{e(t'-1)}{t-1} \right),$$

where $e \approx 2.718$ is Euler's number. The last inequality does not imply that the limit of the sequence \bar{C}_t , $t \geq 0$ exists.

4. From (8) it follows immediately that a sequence $\{\bar{C}_t - \bar{C}_{t+1}\}_{t \geq 0}$ converges to zero as $t \rightarrow \infty$.

Remark 2 The proof of Proposition 2 implies that \bar{C}_t , $t \geq 0$ is not a monotone sequence. Monte Carlo simulation shows that \bar{C}_t tends to zero as $t \rightarrow \infty$, see Fig. 5.

We cannot extend Prop. 2 to graphs such that a node or an edge can be deleted at each step of the CA evolution in a similar way. The reason is the following. If an edge between some nodes $i, i' \in V_t$ (or one of the nodes) is deleted, one has to take into account how this deletion affects on the rest of the graph.

3.3 Submartingality

We introduce a sequence of σ -algebra's as follows:

$$\mathcal{F}_t = \sigma \{G_0, G_1, \dots, G_t\}, \quad t = 0, 1, 2, \dots$$

Obviously, it holds $\mathcal{F}_t \subset \mathcal{F}_{t'}$ when $t \leq t'$, i.e., the sequence $\mathcal{F}_0, \mathcal{F}_1, \dots$ forms a filtration.

Proposition 3 *Let the assumptions of Prop. 1 be satisfied. Then for any fixed node i , the sequence $(k_{i,0}, \mathcal{F}_0), (k_{i,1}, \mathcal{F}_1), \dots$ is a submartingale.*

Proposition 4 *Let the assumptions of Prop. 1 be satisfied. Then for any fixed node i , the sequence $(\Delta_{i,0}, \mathcal{F}_0), (\Delta_{i,1}, \mathcal{F}_1), \dots$ is a submartingale.*

Let us recall that the total count of triangles in the graph G_n is defined by

$$\Delta_t = \frac{1}{3} \sum_{i \in V_t} \Delta_{i,t}. \quad (9)$$

Corollary 2 *Let the assumptions of Prop. 1 be satisfied. Then the sequence*

$$(\Delta_0, \mathcal{F}_0), (\Delta_1, \mathcal{F}_1), \dots$$

is a submartingale.

4 Simulation study

Our simulation study aims to support the theoretical results obtained in Prop. 2-4 for the $CA^{\alpha, \epsilon}$ model without node and edge deletion and to investigate the CA evolution with a uniform node or edge deletion.

Let $G_t = (V_t, E_t)$ be the graph at evolution step t . We consider the CA evolution with the creation of $m_0 \geq 2$ new edges at each evolution step when a new node is appended.

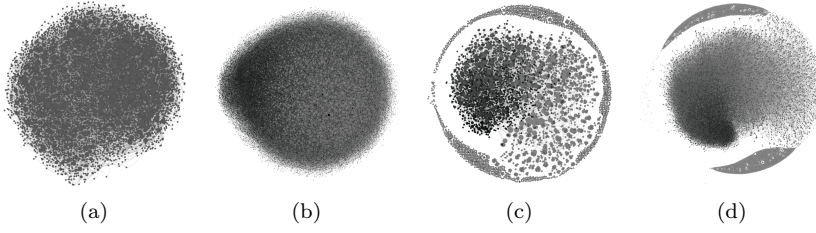


Fig. 1 The graph obtained by the CA with attachment probability (1) and parameters $(\alpha, \epsilon) = (1, 0)$ and $m_0 = 2$ from the initial graph in Fig. 1(a) after $5 \cdot 10^4$ evolution steps without node and edge deletion (Fig. 1(b)), with a uniform node deletion (Fig. 1(c)) and with a uniform edge deletion (Fig. 1(d)). The node size is proportional to the node degree, and the node color represents the "life time" of the node, i.e. the "older" the node the darker the color.

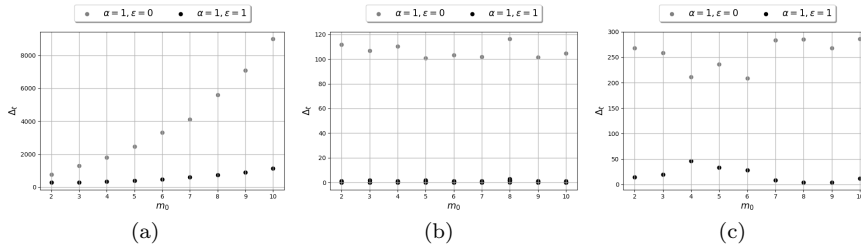


Fig. 2 Averages of total triangle counts Δ_t over 10 graphs against m_0 for the CA graphs after $t = 5 \cdot 10^4$ evolution steps with sets of parameters $(\alpha, \epsilon) \in \{(1, 0), (1, 1)\}$ without node and edge deletion (Fig. 2(a)), with a uniform node deletion (Fig. 2(b)) and with a uniform edge deletion (Fig. 2(c)).

4.1 Illustration of the CA evolution with and without node and edge deletion

An example of an initial graph G_0 obtained by the CA with parameters $m_0 = 2$, $(\alpha, \epsilon) = (1, 0)$ starting from a triangle of connected nodes and containing $5 \cdot 10^3$ nodes is shown in Fig. 1(a). The evolution without node and edge deletion leads to nodes with a dense structure, see Fig. 1(b). A uniform node or edge deletion at each evolution step when a new node and new edges are appended, causes the appearance of isolated nodes. The proportion of the latter nodes is 31.4% and 26.3% for uniform node and edge deletion in Fig. 1(c), 1(d), respectively. Naturally, 'the removal of a node implies the malfunctioning of all its edges as well, node removal inflicts more damage than edge removal' (Albert & Barabási, 2002). If nodes are isolated, then the attachment to them is unlikely since their triangle counts are zero-valued.

4.2 Averaging of total triangle counts

Fig. 2(a) shows that the mean triangle counts grow with increasing m_0 for the CA model without node and edge deletion for both pairs of parameters $(\alpha, \epsilon) \in \{(1, 0), (1, 1)\}$. The case $(1, 0)$ provides a higher increasing rate than $(1, 1)$ since the impact of the clustering coefficient for $(1, 1)$ is by (1) weaker than for $(1, 0)$ and node i can likely get a new edge uniformly irrespective of the number of triangles involving this node. In contrast, the evolution with node or edge deletion in Fig. 2(b), 2(c) leads to a fluctuation around constants for the average triangle counts. For $(\alpha, \epsilon) = (1, 1)$ the triangles appear rarely or they are absent in the graph for any considered values of m_0 . For $(\alpha, \epsilon) = (1, 0)$ the triangle counts are approximately constant with regard to m_0 , and their values are larger for the evolution with edge deletion rather than for the evolution with node deletion.

4.3 The extreme value index estimation

(α, ϵ)	The evolution								
	without node/edge deletion			with node deletion			with edge deletion		
	$\ V_t\ $	$\{k_i > 2\}$	$\{\Delta_{i,t} > 0\}$	$\ V_t\ $	$\{k_i > 0\}$	$\{\Delta_{i,t} > 0\}$	$\ V_t\ $	$\{k_i > 0\}$	$\{\Delta_{i,t} > 0\}$
(1, 0)	55000	1277	1277	5000	125	125	55000	624	624
(1, 1)	55000	36757	311	5000	4596	2	55000	5469	0

Table 1 The number of nodes $\|V_t\|$ after $t = 5 \cdot 10^4$ evolution steps, where the initial graph in Fig. 1(a) contains $5 \cdot 10^3$ nodes; the number of nodes with degrees larger than the minimum value, i.e. $\{k_{i,t} > k_{min}\}$, $k_{min} \in \{0, 2\}$; and the number of nodes involved in triangles for the CA graphs, i.e. such that $\{\Delta_{i,t} > 0\}$ for parameters $(\alpha, \epsilon) \in \{(1, 0), (1, 1)\}$, $m_0 = 2$.

It is claimed in Bagrow and Brockmann (2012) that networks evolving by the CA exhibit an exponential tail of the node degree distribution, i.e. the EVI of the node degree distribution is equal to zero. In order to verify this claim we apply the moment, the mixed moment and the UH estimators, see (Dekkers et al., 1989; Fraga Alves et al., 2009; Beirlant et al., 2004), respectively. The latter semiparametric estimators are designed to estimate real-valued EVI. They are defined by means of the Hill's estimator

$$\hat{\gamma}^H(n, k) = \frac{1}{k} \sum_{i=1}^k \ln \left(\frac{X_{(n-i+1)}}{X_{(n-k)}} \right)$$

built by the order statistics $X_{(1)} \leq X_{(2)} \leq \dots \leq X_{(n)}$ of the observations and for some $k = 1, \dots, n - 1$ (Hill, 1975). The moment estimator is defined as

$$\hat{\gamma}_{n,k}^M = \hat{\gamma}^H(n, k) + 1 - \frac{1}{2} \left(1 - (\hat{\gamma}^H(n, k))^2 / S_{n,k} \right)^{-1},$$

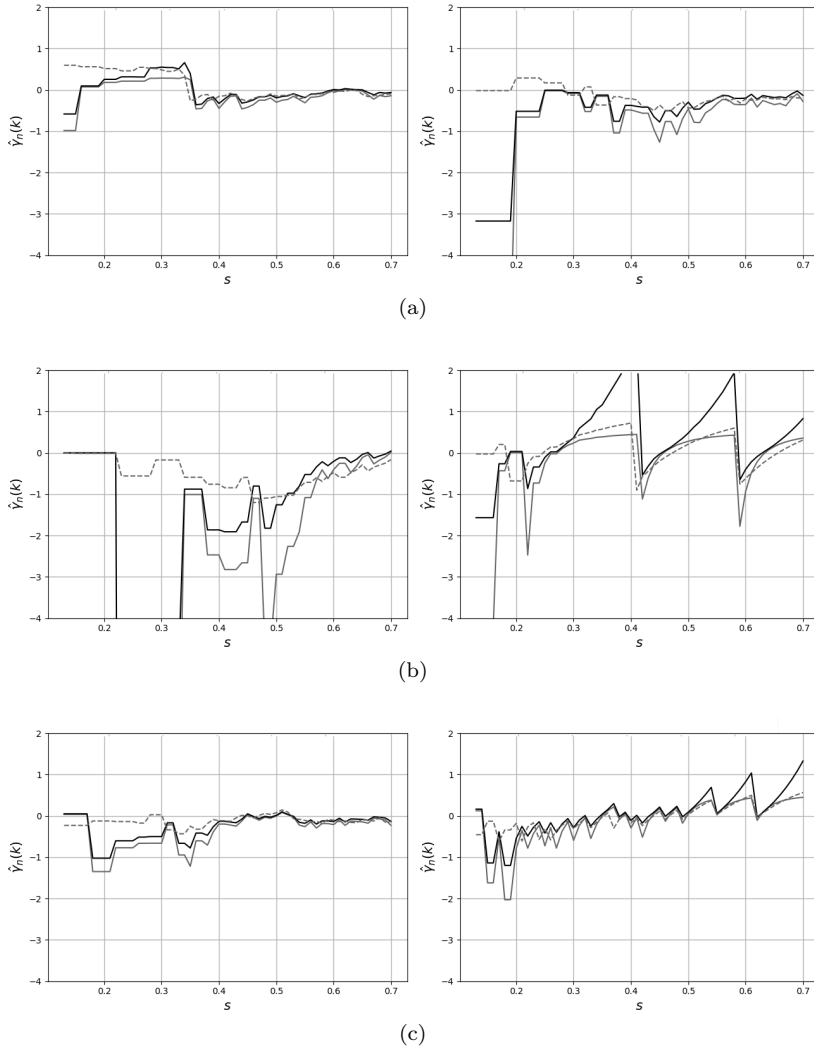


Fig. 3 EVI plots of the moment (grey line), mixed moment (black line) and UH (dotted line) estimates $\hat{\gamma}_n(k)$ of node degrees against the parameter s included in the number of the largest order statistics $k = \lceil n^s \rceil$, $n = \|V_t\|$, for graphs evolved by the CA with probability (1) and parameters $(\alpha, \epsilon) = (1, 0)$ (the left column), and $(\alpha, \epsilon) = (1, 1)$ (the right column) and with $m_0 = 2$ after $t = 5 \cdot 10^4$ evolution steps without node and edge deletion (Fig. 3(a)), with a uniform node deletion (Fig. 3(b)) and with a uniform edge deletion (Fig. 3(c)).

where $S_{n,k} = (1/k) \sum_{i=1}^k (\log X_{(n-i+1)} - \log X_{(n-k)})^2$. The UH estimator is

$$\hat{\gamma}_{n,k}^{UH} = (1/k) \sum_{i=1}^k \log UH_i - \log UH_{k+1},$$

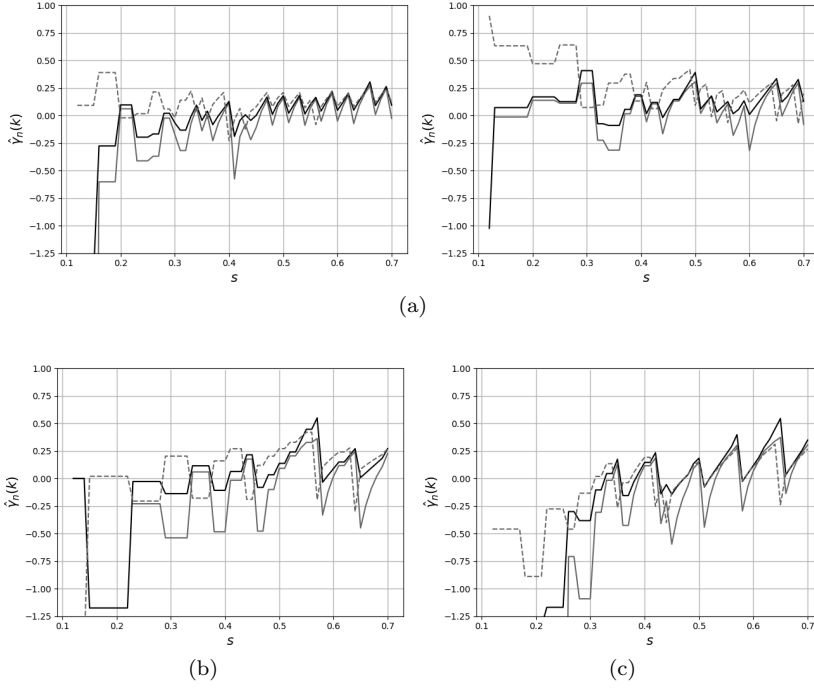


Fig. 4 EVI plots of the moment (grey line), mixed moment (black line) and UH (dotted line) estimates $\hat{\gamma}_n(k)$ of node triangle counts against the parameter s included in the number of the largest order statistics $k = \lceil n^s \rceil$, $n = \|V_t\|$, for graphs evolved by the CA with probability (1) and $m_0 = 2$ after $t = 5 \cdot 10^4$ evolution steps without node and edge deletion (Fig. 4(a)), with a uniform node deletion (Fig. 4(b)) and with a uniform edge deletion (Fig. 4(c)). Parameters (α, ϵ) are equal to $(1, 0)$ (left) and to $(1, 1)$ (right) in Fig. 4(a), and to $(1, 0)$ both in Fig. 4(b), 4(c).

where $UH_i = X_{(n-i)} \hat{\gamma}^H(n, i)$. The mixed moment estimator is defined as

$$\hat{\gamma}_n^{MM}(k) = \frac{\hat{\varphi}_n(k) - 1}{1 + 2 \min(\hat{\varphi}_n(k) - 1, 0)},$$

where

$$\hat{\varphi}_n(k) = \frac{\hat{\gamma}^H(n, k) - L_n^{(1)}(k)}{\left(L_n^{(1)}(k)\right)^2}, \quad L_n^{(1)}(k) = 1 - \frac{1}{k} \sum_{i=1}^k \frac{X_{(n-k)}}{X_{(n-i+1)}}.$$

By one of the oldest empirical rule, one can take any first values $\hat{\gamma}_n(\lceil n^s \rceil)$, $0 < s < 1$ corresponding to the most left stability interval of the Hill's plot as the estimate of the EVI. One can find k by the bootstrap method (Markovich, 2007).

We simulate two graphs evolving by the CA with parameters $(\alpha, \epsilon) = (1, 0)$ and $(\alpha, \epsilon) = (1, 1)$. To estimate EVI of node degrees we exclude from

the data nodes with the minimum degree equal to $k_{min} = m_0 = 2$ for the evolution without node and edge deletion. There are no isolated nodes but a large number of nodes that have two edges $k_i = 2$ in this case. We remove isolated nodes with zero node degree $k_{min} = 0$ for the evolution with node or edge deletion. Nodes with zero triangle counts are excluded to estimate EVI of triangle counts. In Tab. 1 one can see the number of non-excluded observations.

By Fig.3 one can conclude that the EVIs of node degrees are close to zero irrespective of the strategies of node and edge removal. This implies that the distribution tails of the node degrees are light-tailed. The same may be concluded for triangle counts, see Fig. 4. The case $(\alpha, \epsilon) = (1, 1)$ for the CA evolution with node or edge deletion is not shown in Fig. 4 due to the lack of triangles in the graphs.

4.4 Simulation of the $CA^{(\alpha, \epsilon)}$ model

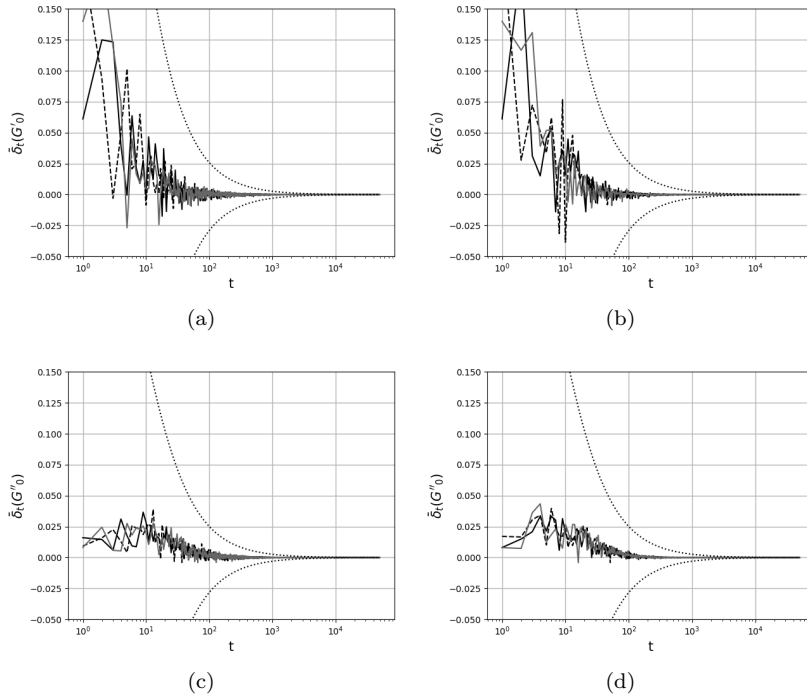


Fig. 5 Plots of $\bar{\delta}_t(G_0)$ with bounds (8) shown by dotted lines for initial graphs G'_0 (Fig. 5(a), 5(b)) and G''_0 (Fig. 5(c), 5(d)): $CA^{(\alpha, \epsilon)}$ is provided for $\alpha \in \{0.5, 1, 2\}$ (dark, dashed dark and grey lines, respectively) and $\epsilon \in \{0, 1\}$ (left and right columns, respectively).

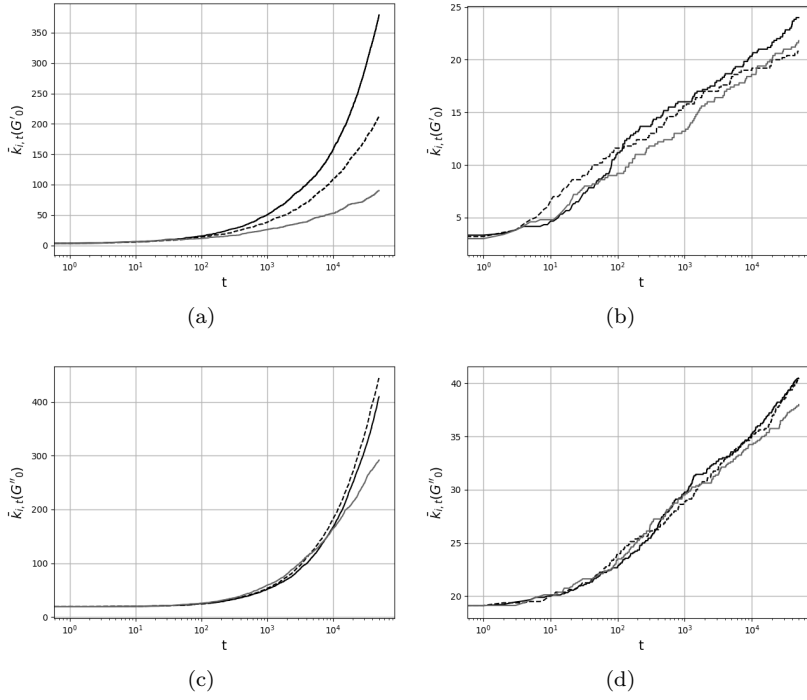


Fig. 6 Plots of $\bar{k}_{i,t}(G_0)$ for initial graphs G'_0 (Fig. 6(a),6(b)) and G''_0 (Fig. 6(c),6(d)) and for $CA(\alpha, \epsilon)$ with $\alpha \in \{0.5, 1, 2\}$ (solid, dashed and grey lines, respectively) and $\epsilon \in \{0, 1\}$ (left and right columns, respectively).

Let us confirm the theoretical results of Section 3. To this end, we simulate 20 samples of graphs of size $5 \cdot 10^4$ by the $CA^{(\alpha, \epsilon)}$ model with $m_0 = 2$, $\alpha \in \{0.5, 1, 2\}$, $\epsilon \in \{0, 1\}$ starting with a triangle G'_0 or an icosahedron with all its diagonals G''_0 as an initial graph G_0 . The CA model is considered without node and edge deletion. We investigate deviations of the average clustering coefficient $\bar{C}_t - \bar{C}_{t+1}$, the mean node degree $E[k_{i,t}]$ and the mean triangle counts $E[\Delta_{i,t}]$ of the i th node by the corresponding sample means over 20 graphs

$$\bar{\delta}_t(G_0) = \frac{1}{20} \sum_{j=1}^{20} (\bar{C}_t^{(j)} - \bar{C}_{t+1}^{(j)}), \bar{k}_{i,t}(G_0) = \frac{1}{20} \sum_{j=1}^{20} k_{i,t}^{(j)}, \bar{\Delta}_{i,t}(G_0) = \frac{1}{20} \sum_{j=1}^{20} \Delta_{i,t}^{(j)}$$

to support Prop. 2-4. The node i is taken as one of the nodes of G'_0 and G''_0 due to the symmetry. We aim also to investigate the impact of the initial graphs on statements of Prop. 2-4.

Convergence of $\bar{\delta}_t(G_0)$ to zero with the time irrespective of the values (α, ϵ) is shown in Fig. 5 that is in agreement with Prop. 2. One can see that the impact of G'_0 and G''_0 is weakened after 100 evolution steps.

The increasing of $\bar{k}_{i,t}(G_0)$ as t grows in Fig. 6 is in agreement with Prop. 3.

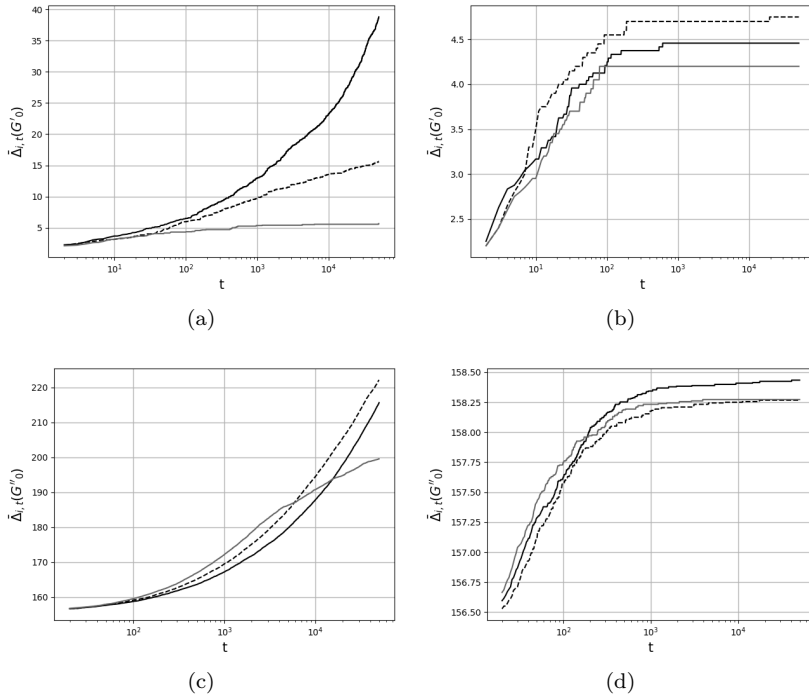


Fig. 7 Plots of $\bar{\Delta}_{i,t}(G_0)$ for initial graphs G'_0 (Fig. 6(a),6(b)) and G''_0 (Fig. 6(c),6(d)) and for $CA(\alpha, \epsilon)$ with $\alpha \in \{0.5, 1, 2\}$ (solid, dashed and grey lines, respectively) and $\epsilon \in \{0, 1\}$ (left and right columns, respectively).

For $\epsilon = 1$ the impact of G_0 on $\bar{k}_{i,t}(G_0)$ is not significant since the attachment probability (1) is determined mostly by ϵ and the attachment probability is close to uniform. However, for $\epsilon = 0$ when the attachment probability (1) depends on the clustering coefficients $c_{i,t}$ only, the rate of the increase is as faster as smaller α and larger G_0 are. The increasing of $\bar{k}_{i,t}(G_0)$ is nearly linear for $\epsilon = 1$ and it proceeds as an exponential functions for $\epsilon = 0$.

In Fig. 7 the correspondence of $\bar{\Delta}_{i,t}(G_0)$ to Prop. 4 and its dependence on G_0 are investigated. For G'_0 the number of triangles is smaller than for G''_0 . For $\epsilon = 1$ all curves are similar irrespective on the values of α and reach stable levels rather quickly. For $\epsilon = 0$ and $\alpha = 2$ $\bar{\Delta}_{i,t}(G_0)$ tends to a constant as t increases. In fact, the increasing rates differ for G'_0 and G''_0 and for $\epsilon = 0$.

5 Real network analysis

5.1 Transport networks

We consider the following transport networks: the Flight network from register (Poursafaei et al., 2022; Strohmeier et al., 2021) and the Multilayer Tempo-

ral Network of Public Transport in Great Britain (MLPTGB) (Gallotti & Barthelemy, 2015). The number of nodes in these networks is fixed. The evolution occurs in a change in the number of edges between nodes.

There are 13169 nodes in the Flight network that correspond to the largest world airports which have accepted 3573482 flights during 121 days in year 2019. A flight between airports can be interpreted as the edge. Three airports between which there are flights per day are taken as triangles of nodes. The number of flights from an airport i to other airports is interpreted as the degree of node i . In Poursafaei et al. (2022), the direction of connections (flights) is neglected. A more complete sample of flights is presented in Strohmeier et al. (2021), Olive et al. (2022). Since there can be several flights per day between two airports, they may be described by parallel edges, which are counted as one edge when counting the number of triangles. If there were no flights between airports, then this is considered as the removal of edges between nodes. Nodes-airports are not deleted.

The MLPTGB contains timetable data obtained from the United Kingdom open-data program together with timetables of domestic flights, and obtains a comprehensive snapshot of the temporal characteristics of the whole UK public transport system for a week in October 2010. The data are collected every minute. Different transport modes such as connections at airports, ferry docks, rail, metro, coach and bus stations are included with 262384 nodes in total. The dataset describes the public transport network of Great Britain by using a multilayer node-list and edge-list, where each layer is associated to a single transport mode. Each node is geo-referenced, thus defining a spatial network. 134710018 edges are directed and they represent transport routes between the locations currently in use. The edges can be either intra-layer, between different nodes in the same layer, or inter-layer, between the same node in different layers. Further in the work, the direction of edges is neglected as for the Flight network.

In Fig. 8, node degrees $k_{i,t}$, triangle counts $\Delta_{i,t}$ of nodes $i \in \{i_1, i_2, i_3\}$, and the deviation of the clustering coefficients averaging by all nodes $\delta_t = \bar{C}_t - \bar{C}_{t+1}$ are shown. The node i_1 is the transport hub with the largest number of flights/transfers within the whole observation time. Nodes i_2 and i_3 are ranked as the 100th and 1000th largest transport nodes, respectively. $k_{i,t}$ and $\Delta_{i,t}$ increase, and δ_t fluctuates around zero for both networks. For the Flight network the increase rate of $k_{i,t}$ and $\Delta_{i,t}$ is slower about $t = 20$ due to COVID restrictions and the decrease of the air traffic. For the MLPTGB network, the increase is not quite linear due to a periodic behavior of $k_{i,t}$ and $\Delta_{i,t}$ between a middle day activity and night-sleeping levels. The activity is weaker at weekend which also reflects on $k_{i,t}$, $\Delta_{i,t}$ and δ_t . The triangle counts are stabilized which can be explained by the logistic.

Tab. 2 shows that $\{\Delta_{i,t}\}$ and $\{k_{i,t}\}$ are heavy-tailed distributed due to positive estimates of γ for the Flight network. However, γ estimates are close to zero or negative for the MLPTGB network which indicate light-tailed distributions of $\{\Delta_{i,t}\}$ and $\{k_{i,t}\}$. One can suggest indirectly that the Flight network may evolve by the linear PA and the MLPTGB network by the CA.

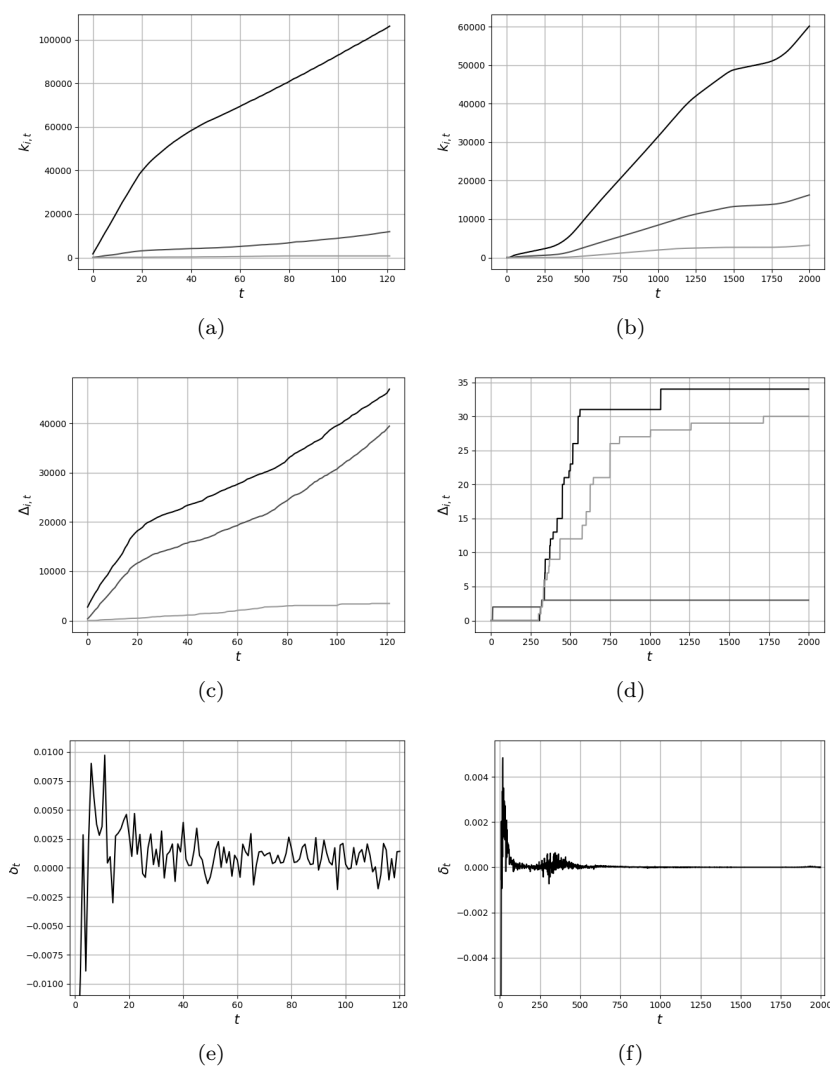


Fig. 8 Plots of $k_{i,t}$, $\Delta_{i,t}$ of nodes $i \in \{i_1, i_2, i_3\}$ shown by black, dark-grey and grey lines, and δ_t for the Flight network (left column) and the MLPTGB network (right column) against t in days.

5.2 Face-to-face (F2F) proximity data

To understand contacts between children at school and quantify the transmission opportunities of respiratory infections, measurements carried out in a French school (6–12 years children) were collected on Thursday, October 1st and Friday, October 2nd 2009 between 8 : 30 *am* and 3 *p.m.* o'clock. We consider the data on the time-resolved face-to-face proximity of children and

Table 2 The estimation of the EVI γ of node degrees $\{k_{i,t}\}$ and triangle counts $\{\Delta_{i,t}\}$ for real networks.

Network	MM estimate		M estimate		UH estimate	
	$\{k_{i,t}\}$	$\{\Delta_{i,t}\}$	$\{k_{i,t}\}$	$\{\Delta_{i,t}\}$	$\{k_{i,t}\}$	$\{\Delta_{i,t}\}$
Flight	0.282	0.187	0.252	0.442	0.224	0.377
MLPTGB	0.098	0.1	-0.006	0.075	-0.013	0.111
F2F	-0.149	-0.045	-0.56	-0.413	-0.291	-0.227

teachers based on radio frequency identification devices provided in Stehlé et al. (2011). 77602 contact events between 242 individuals (232 children and 10 teachers) were recorded. The data are available at www.sociopatterns.org/datasets/primary-school-temporal-network-data/. Similar investigation of the contacts of children at school and the propagation of many infectious diseases in the community is considered in Gemmetto et al. (2014). The temporal evolution of the contact network and the trajectories followed by the children in the school, which constrain the contact patterns is mentioned in Bagrow and Brockmann (2012) as an example of the CA evolution.

Considering each participant of the experiment as a graph node and one continuous contact between two people as an edge, we provide the same analysis as for the transport networks. There can be parallel edges in the case of multiple contacts between two persons.

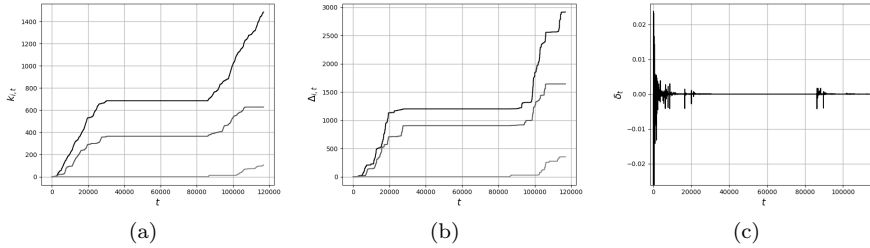


Fig. 9 Plots of $k_{i,t}$, $\Delta_{i,t}$ of nodes $i \in \{i_1, i_2, i_3\}$ shown by black, dark-grey and grey lines, and δ_t for the F2F network against t in sec.

In Fig. 9, the same characteristics as in Fig. 8 are presented. The nodes i_1 and i_2 represent the most and the average contact pupils. The node i_3 is a pupil who missed the first day and was the least contact at the second day. The stability intervals in Fig. 9(a), 9(b) correspond to the time outside of the school when contact measurements were not performed. $k_{i,t}$ and $\Delta_{i,t}$ increase for all persons. In Fig. 9(c), δ_t stabilizes at zero over the time. Tab. 2 shows that $\{\Delta_{i,t}\}$ and $\{k_{i,t}\}$ are light-tailed distributed for the F2F network due to negative values of the γ estimates.

6 Conclusions

The evolution of undirected graphs generated by the CA model without node and edge deletion and with a uniform node or edge deletion is studied. Theoretical results are obtained for the CA model without node and edge deletion and when a newly appended node is connected to two existing nodes of the graph at each evolution step. The simulation study is provided also for the CA model with a uniform node or edge deletion.

We obtain the following theoretical properties of the $CA^{(\alpha, \epsilon)}$ model, $\alpha, \epsilon > 0$: (1) by Proposition 2 the sequence of increments of the consecutive mean clustering coefficients tends to zero; (2) by Propositions 3, 4 the sequences of node degrees and triangle counts of any fixed node are submartingales with respect to the filtration $\mathcal{F}_t = \sigma\{G_0, G_1, \dots, G_t\}$, $t = 0, 1, 2, \dots$. The both results were obtained for any initial graph. The first item is valid for any CA or PA model.

The following phenomena of the $CA^{(\alpha, \epsilon)}$ model, $\alpha > 0$, $\epsilon > 0$ are approved by the simulation study: (1) the CA leads to light-tailed distributed node degrees and triangle counts irrespective of the deletion strategies and the considered values of the parameters (α, ϵ) of the CA model; (2) the average clustering coefficient tends to a constant in time irrespective of the choice of an initial graph and the values of the parameters (α, ϵ) ; (3) the mean node degree and the mean triangle count increase over time and the rate of increasing depends on the parameter ϵ : as smaller ϵ is as more visible the impact of the choice of the initial graph G_0 is.

Our future research may concern to a random parameter m_0 . Theoretical results can be extended to the cases of a node and edge deletion.

A Proof of Proposition 1

Proof Let us introduce random events

$$A_i = \{\text{node } i \text{ is chosen}\}, \quad i \in V_t.$$

Then we have $P(W_t = \{i, j\}) = P(A_i \cap A_j)$. By the law of total probability, it holds

$$\begin{aligned} P(A_i \cap A_j) &= P(A_i|A_j)P(A_j) + P(A_j|A_i)P(A_i) \\ &= \frac{P_{CA}(i, t)}{1 - P_{CA}(j, t)} \cdot P_{CA}(j, t) + \frac{P_{CA}(j, t)}{1 - P_{CA}(i, t)} \cdot P_{CA}(i, t). \end{aligned}$$

B Proof of Corollary 1

Proof Let us consider the case $\epsilon > 0$. From (6) it follows that $0 \leq P(W_t = \{i, j\}) \leq 1$ for any $\{i, j\} \in \mathcal{E}_t$. Thus, the proof will be ended if we show that

$$\sum_{\{i, j\} \in \mathcal{E}_t} P(W_t = \{i, j\}) = 1. \quad (10)$$

Assume, without loss of generality, that $i < j$. From the Introduction we know that $\|V_t\| = \|V_0\| + t$. Thus,

$$\sum_{\{i,j\} \in \mathcal{E}_t} P(W_t = \{i,j\}) = \sum_{i=1}^{\|V_0\|+t-1} \sum_{j=i+1}^{\|V_0\|+t} P(W_t = \{i,j\}). \quad (11)$$

The left hand side of (11) is equal to the sum $S_{1,t} + S_{2,t}$, where

$$\begin{aligned} S_{1,t} &= \sum_{i=1}^{\|V_0\|+t-1} P_{CA}(i,t) \sum_{j=i+1}^{\|V_0\|+t} \frac{P_{CA}(j,t)}{1 - P_{CA}(j,t)}, \\ S_{2,t} &= \sum_{i=1}^{\|V_0\|+t-1} \frac{P_{CA}(i,t)}{1 - P_{CA}(i,t)} \sum_{j=i+1}^{\|V_0\|+t} P_{CA}(j,t). \end{aligned}$$

We change the summation order to get

$$\begin{aligned} S_{1,t} &= \sum_{j=2}^{\|V_0\|+t} \frac{P_{CA}(j,t)}{1 - P_{CA}(j,t)} \sum_{i=1}^{j-1} P_{CA}(i,t) \\ &= P_{CA}(\|V_0\| + t, t) + \sum_{j=2}^{\|V_0\|+t-1} \frac{P_{CA}(j,t)}{1 - P_{CA}(j,t)} \sum_{i=1}^{j-1} P_{CA}(i,t). \end{aligned}$$

Regarding the sum $S_{2,t}$ we rewrite it as follows:

$$S_{2,t} = P_{CA}(1,t) + \sum_{i=2}^{\|V_0\|+t-1} \frac{P_{CA}(i,t)}{1 - P_{CA}(i,t)} \sum_{j=i+1}^{\|V_0\|+t} P_{CA}(j,t).$$

Putting $S_{1,t}$ and $S_{2,t}$ together we obtain

$$S_{1,t} + S_{2,t} = \sum_{i=1}^{\|V_0\|+t} P_{CA}(i,t) = 1.$$

This ends the proof of (10) and the case $\epsilon > 0$ as well. The proof of the case $\epsilon = 0$ is similar and, thus, it is omitted.

C Proof of Proposition 2

Proof Since $m_0 = 2$, the newly appended node $\|V_0\| + t + 1$ is connected with some pair of nodes $j_1, j_2 \in V_t$. As for the rest of the nodes $\nu \in V_t \setminus \{j_1, j_2\}$, we have $c_{\nu, t+1} = c_{\nu, t}$. We rewrite \bar{C}_{t+1} as follows:

$$\bar{C}_{t+1} = \frac{c_{j_1, t+1} + c_{j_2, t+1} + c_{\|V_0\|+t+1, t+1}}{\|V_0\| + t + 1} + \frac{1}{\|V_0\| + t + 1} \sum_{\nu \in V_{t+1} \setminus \{j_1, j_2, \|V_0\|+t+1\}} c_{\nu, t+1}.$$

Note that $V_{t+1} \setminus \{j_1, j_2, \|V_0\| + t + 1\} = V_t \setminus \{j_1, j_2\}$. By adding $c_{j_1, t}/(\|V_0\| + t + 1)$ and $c_{j_2, t}/(\|V_0\| + t + 1)$ to the last sum we obtain

$$\bar{C}_{t+1} = \frac{(c_{j_1, t+1} - c_{j_1, t}) + (c_{j_2, t+1} - c_{j_2, t}) + c_{\|V_0\|+t+1, t+1}}{\|V_0\| + t + 1} + \frac{\|V_0\| + t}{\|V_0\| + t + 1} \bar{C}_t,$$

and consequently,

$$\begin{aligned} \bar{C}_t - \bar{C}_{t+1} &= -\frac{(c_{j_1,t+1} - c_{j_1,t}) + (c_{j_2,t+1} - c_{j_2,t}) + c_{\|V_0\|+t+1,t+1}}{\|V_0\| + t + 1} \\ &\quad + \frac{1}{\|V_0\| + t + 1} \bar{C}_t. \end{aligned} \quad (12)$$

We consider two cases: (a) nodes j_1 and j_2 are disconnected; (b) nodes j_1 and j_2 are connected.

Case (a). Since nodes j_1 and j_2 are disconnected, we have $c_{\|V_0\|+t+1,t+1} = 0$ and

$$c_{\nu,t+1} = \begin{cases} 0, & k_{\nu,t} \leq 1, \\ ((k_{\nu,t} - 1)/(k_{\nu,t} + 1))c_{\nu,t}, & k_{\nu,t} \geq 2, \end{cases} \quad \nu \in \{j_1, j_2\}.$$

Let $k_{\nu,t} \leq 1$, $\nu \in \{j_1, j_2\}$ hold. Then we get $\bar{C}_t - \bar{C}_{t+1} = \bar{C}_t/(\|V_0\| + t + 1)$. Whence, by using a rough bound $\bar{C}_t \leq 1$ we get

$$0 < \bar{C}_t - \bar{C}_{t+1} \leq \frac{1}{\|V_0\| + t + 1}. \quad (13)$$

Let us consider the case $k_{j_1,t} \geq 2$ and $k_{j_2,t} \leq 1$. Then we have

$$\bar{C}_t - \bar{C}_{t+1} = \frac{2c_{j_1,t}}{(k_{j_1,t} + 1)(\|V_0\| + t + 1)} + \frac{1}{\|V_0\| + t + 1} \bar{C}_t.$$

Now we use $\bar{C}_t \leq 1$, $c_{j_1,t} \leq 1$ and $k_{j_1,t} \geq 2$ to get

$$0 < \bar{C}_t - \bar{C}_{t+1} \leq \frac{5/3}{\|V_0\| + t + 1}. \quad (14)$$

Let $k_{j_1,t} \leq 1$ and $k_{j_2,t} \geq 2$. Then (14) holds. It is easy to check that we derive the inequality

$$0 < \bar{C}_t - \bar{C}_{t+1} \leq \frac{7/3}{\|V_0\| + t + 1} \quad (15)$$

in the case $k_{j_1,t} \geq 2$ and $k_{j_2,t} \geq 2$.

Case (b). Let nodes j_1 and j_2 be connected. Then we have $c_{\|V_0\|+t+1,t+1} = 1$ and

$$c_{\nu,t+1} = \begin{cases} 1, & k_{\nu,t} = 1, \\ ((k_{\nu,t} - 1)/(k_{\nu,t} + 1))c_{\nu,t} + 2/(k_{\nu,t}(k_{\nu,t} + 1)), & k_{\nu,t} \geq 2, \end{cases} \quad (16)$$

where $\nu \in \{j_1, j_2\}$.

Let $k_{\nu,t} = 1$, $\nu \in \{j_1, j_2\}$ hold. This implies $c_{\nu,t} = 0$ and $c_{\nu,t+1} = c_{\|V_0\|+t+1,t+1} = 1$, $\nu \in \{j_1, j_2\}$. Thus, by (12) we have

$$\bar{C}_t - \bar{C}_{t+1} = -\frac{3}{\|V_0\| + t + 1} + \frac{1}{\|V_0\| + t + 1} \bar{C}_t.$$

It yields

$$-\frac{3}{\|V_0\| + t + 1} \leq \bar{C}_t - \bar{C}_{t+1} \leq -\frac{2}{\|V_0\| + t + 1} \quad (17)$$

due to $\bar{C}_t \leq 1$.

Let $k_{j_1,t} \geq 2$ and $k_{j_2,t} = 1$ hold. We have $c_{j_2,t} = 0$ and $c_{j_2,t+1} = 1$. By (16) it follows

$$c_{j_1,t+1} - c_{j_1,t} = \frac{2}{k_{j_1,t} + 1} \left(\frac{1}{k_{j_1,t}} - c_{j_1,t} \right). \quad (18)$$

By (12) and (18) it follows

$$\bar{C}_t - \bar{C}_{t+1} = -\frac{2((1/k_{j_1,t} - c_{j_1,t})/(k_{j_1,t} + 1) + 1)}{\|V_0\| + t + 1} + \frac{1}{\|V_0\| + t + 1} \bar{C}_t.$$

Since $0 \leq c_{j_1,t} \leq 1$ and $k_{j_1,t} \geq 2$ holds, we get

$$\frac{1}{k_{j_1,t} + 1} (1/k_{j_1,t} - c_{j_1,t}) + 1 \geq 1 - \frac{1}{k_{j_1,t} + 1} \geq \frac{2}{3}. \quad (19)$$

We claim that

$$\frac{1}{k_{j_1,t} + 1} (1/k_{j_1,t} - c_{j_1,t}) + 1 \leq \frac{7}{6}. \quad (20)$$

The inequality (20) is equivalent to $c_{j_1,t} \geq 1/k_{j_1,t} - (k_{j_1,t} + 1)/6$. The right-hand side of the latter inequality is strictly decreasing on the negative half-axis by $k_{j_1,t} \geq 2$ and it equals to zero when $k_{j_1,t} = 2$. Then we get

$$-\frac{7/3}{\|V_0\| + t + 1} \leq \bar{C}_t - \bar{C}_{t+1} \leq -\frac{1/3}{\|V_0\| + t + 1}. \quad (21)$$

One can check that inequalities (21) hold under the assumptions $k_{j_1,t} = 1$ and $k_{j_2,t} \geq 2$.

Let us assume that $k_{j_1,t} \geq 2$ and $k_{j_2,t} \geq 2$ hold. The relations (12) and (18) lead to the following

$$\begin{aligned} \bar{C}_t - \bar{C}_{t+1} = & -\frac{1}{\|V_0\| + t + 1} \left(\frac{2}{(k_{j_1,t} + 1)k_{j_1,t}} - \frac{2c_{j_1,t}}{k_{j_1,t} + 1} \right. \\ & \left. + \frac{2}{(k_{j_2,t} + 1)k_{j_2,t}} - \frac{2c_{j_2,t}}{k_{j_2,t} + 1} + 1 \right) + \frac{\bar{C}_t}{\|V_0\| + t + 1}. \end{aligned}$$

By combining (19) and (20) we get

$$-\frac{1}{6} \leq \frac{2}{(k_{\nu,t} + 1)k_{\nu,t}} - \frac{2c_{\nu,t}}{k_{\nu,t} + 1} + \frac{1}{2} \leq \frac{5}{6}, \quad \nu \in \{j_1, j_2\}.$$

The last inequalities, together with $0 \leq \bar{C}_t \leq 1$, give

$$-\frac{5/3}{\|V_0\| + t + 1} \leq \bar{C}_t - \bar{C}_{t+1} \leq \frac{4/3}{\|V_0\| + t + 1}. \quad (22)$$

Summarizing the inequalities (13)-(15), (17), (21) and (22) we get (8).

D Proof of Proposition 3

Proof There are two cases: the node number i satisfies either the inequality $1 \leq i \leq \|V_0\|$, or

$$i > \|V_0\|. \quad (23)$$

The consideration of both cases is similar. Thus, we prove the statement for (23), only.

From (23) it follows that there exists a unique natural t , such that $i = \|V_0\| + t$ holds. A constant is measurable with respect to any σ -algebra including a trivial one. Thus, from (7) it follows that the random variable (r.v.) $k_{\|V_0\|+t,s}$ is \mathcal{F}_s -measurable for $0 \leq s \leq t$. The construction of \mathcal{F}_t allows us to conclude that $k_{\|V_0\|+t,s}$ is \mathcal{F}_s -measurable for any $s > t$.

Let us show that for any $s \geq 0$ it holds

$$E(k_{\|V_0\|+t,s+1} | \mathcal{F}_s) \geq k_{\|V_0\|+t,s}. \quad (24)$$

By (7) and $k_{\|V_0\|+t,t} = 2$ we find that (24) holds for $0 \leq s \leq t$. Assume now that $s > t$ holds. Let $p_{\|V_0\|+t,s+1}^{(1)}$ denote the conditional probability that a pair of nodes $\{j_1, j_2\}$, $j_1 \neq j_2$ is chosen from the graph G_s by using the WSwR such that one of the equalities $j_1 = \|V_0\| + t$ or $j_2 = \|V_0\| + t$ holds given that the graph G_s is known. Then, by (6) we get

$$\begin{aligned} p_{\|V_0\|+t,s+1}^{(1)} &= \sum_{j \in V_s \setminus \{\|V_0\|+t\}} P(W_t = \{\|V_0\| + t, j\}) \\ &= \frac{P_{CA}(\|V_0\| + t, s)}{1 - P_{CA}(\|V_0\| + t, s)} \sum_{j \in V_s \setminus \{\|V_0\|+t\}} P_{CA}(j, s) \\ &\quad + P_{CA}(\|V_0\| + t, s) \sum_{j \in V_s \setminus \{\|V_0\|+t\}} \frac{P_{CA}(j, s)}{1 - P_{CA}(j, s)} \\ &= P_{CA}(\|V_0\| + t, s) \left(1 + \sum_{j \in V_s \setminus \{\|V_0\|+t\}} \frac{P_{CA}(j, s)}{1 - P_{CA}(j, s)} \right). \end{aligned}$$

Since

$$\begin{aligned} P(k_{\|V_0\|+t,s+1} - k_{\|V_0\|+t,s} = 1 | \mathcal{F}_s) &= p_{\|V_0\|+t,s+1}^{(1)}, \\ P(k_{\|V_0\|+t,s+1} - k_{\|V_0\|+t,s} = 0 | \mathcal{F}_s) &= 1 - p_{\|V_0\|+t,s+1}^{(1)} \end{aligned}$$

hold and $k_{\|V_0\|+t,s}$ is the \mathcal{F}_s -measurable r.v., we obtain

$$\begin{aligned} E(k_{\|V_0\|+t,s+1} | \mathcal{F}_s) &= E(k_{\|V_0\|+t,s} + (k_{\|V_0\|+t,s+1} - k_{\|V_0\|+t,s}) | \mathcal{F}_s) \\ &= k_{\|V_0\|+t,s} + E(k_{\|V_0\|+t,s+1} - k_{\|V_0\|+t,s} | \mathcal{F}_s) \\ &= k_{\|V_0\|+t,s} + p_{\|V_0\|+t,s+1}^{(1)} \geq k_{\|V_0\|+t,s}. \end{aligned}$$

This ends the proof of (24). It remains to prove that for any $s \geq 0$,

$$E(k_{\|V_0\|+t,s}) < \infty. \quad (25)$$

The inequality (25) for $0 \leq s \leq t$ follows obviously. Let $s > t$. We rewrite $E(k_{\|V_0\|+t,s})$ as the telescopic sum:

$$\begin{aligned} &E(k_{\|V_0\|+t,s}) \\ &= E(k_{\|V_0\|+t,t} + (k_{\|V_0\|+t,t+1} - k_{\|V_0\|+t,t}) + \dots + (k_{\|V_0\|+t,s} - k_{\|V_0\|+t,s-1})) \\ &= 2 + \sum_{j=t+1}^s E(k_{\|V_0\|+t,j} - k_{\|V_0\|+t,j-1}). \end{aligned}$$

By the law of the total probability, we have

$$E(k_{\|V_0\|+t,j} - k_{\|V_0\|+t,j-1}) = E(E(k_{\|V_0\|+t,j} - k_{\|V_0\|+t,j-1} | \mathcal{F}_{j-1})) E(p_{\|V_0\|+t,j}^{(1)}) \leq 1.$$

This gives $E(k_{\|V_0\|+t,s}) \leq 2 + (s - t)$. Thus, (25) follows.

E Proof of Proposition 4

Proof The proposition can be proved by using a similar argument as in the proof of Prop. 3. Here we note only that for $s \geq t$ it holds

$$\begin{aligned} P\left(\Delta_{\|V_0\|+t,s+1} - \Delta_{\|V_0\|+t,s} = 1 | \mathcal{F}_s\right) &= p_{\|V_0\|+t,s+1}^{(2)}, \\ P\left(\Delta_{\|V_0\|+t,s+1} - \Delta_{\|V_0\|+t,s} = 0 | \mathcal{F}_s\right) &= 1 - p_{\|V_0\|+t,s+1}^{(2)}, \end{aligned}$$

where

$$p_{\|V_0\|+t,s+1}^{(2)} = \sum_{\{i,j\} \in \mathcal{D}_{\|V_0\|+t} \cap E_s} P(W_s = \{i,j\})$$

and $\mathcal{D}_{\|V_0\|+t}$ is the set of unordered pairs defined as follows:

$$\mathcal{D}_{\|V_0\|+t} = \{\{\|V_0\| + t, i\} : i \in V_s \setminus \{\|V_0\| + t\}\}.$$

F Proof of Corollary 2

Proof Let us note first that for any $t \geq 0$, Δ_t is a \mathcal{F}_t -measurable r.v. as the finite sum of the \mathcal{F}_t -measurable r.v.s $\{\Delta_{i,t}\}$, $i \in V_t$. Next, by using (9) we derive

$$E(\Delta_{t+1} | \mathcal{F}_t) = \frac{1}{3} \sum_{i \in V_t} E(\Delta_{i,t+1} | \mathcal{F}_t) + E(\Delta_{\|V_0\|+t+1,t+1} | \mathcal{F}_t).$$

Applying Prop. 4 we get

$$E(\Delta_{t+1} | \mathcal{F}_t) \geq \frac{1}{3} \sum_{i \in V_t} \Delta_{i,t} + E(\Delta_{\|V_0\|+t+1,t+1} | \mathcal{F}_t) \geq \Delta_t.$$

Here, we used the fact that $0 \leq \Delta_{\|V_0\|+t+1,t+1} \leq 1$.

One can apply Prop. 4 one more time to verify the inequality $E(\Delta_t) < \infty$, $t \geq 0$.

References

1. Albert, R., Barabási, A.-L. (2002). Statistical mechanics of complex networks. *Rev. Mod. Phys.*, **74**(1), 47-97. <https://doi.org/10.1103/RevModPhys.74.47>
2. Albert, R., Albert, I., Nakarado, G. L. (2004). Structural vulnerability of the North American power grid. *Physical Review E*, **69**, 025103. <https://doi.org/10.1103/PhysRevE.69.025103>
3. Avrachenkov, K., Dreveton, M. (2022). Statistical Analysis of Networks. Boston–Delft: now publishers. <http://dx.doi.org/10.1561/9781638280514>
4. Bagrow, J., Brockmann, D. (2012). Natural Emergence of Clusters and Bursts in Network Evolution. *Physical Review X*, **3**, 021016. DOI: 10.1103/PhysRevX.3.021016
5. Bringmann K., Keusch R. & Lengler J. (2019). Geometric inhomogeneous random graphs. *Theoretical Computer Science*, **760**, 35-54. <https://doi.org/10.1016/j.tcs.2018.08.014>
6. Beirlant, J., Goegebeur, Y., Teugels, J. & Segers, J. (2004). *Statistics of Extremes: Theory and Applications*. Chichester, West Sussex: Wiley.
7. de Haan, L., Ferreira, A. (2007). *Extreme Value Theory: An Introduction* Springer Science and Business Media.
8. Dekkers, A.L.M., Einmahl, J.H.J. & de Haan, L. (1989). A moment estimator for the index of an extreme-value distribution. *Ann. Statist.*, **17**, 1833-1855. <https://www.jstor.org/stable/2241667>

9. Deng, W.B., Guo, L., Li, W., Cai, X. (2009). Worldwide Marine Transportation Network: Efficiency and Container Throughput. *Chinese Physics Letters*, 26(11), 118901. <https://doi.org/10.1088/0256-307X/26/11/118901>
10. Devroye, L. (1986). *Non-Uniform Random Variate Generation*. Springer-Verlag, New-York.
11. Embrechts, P., Kluppelberg, C. and Mikosch, T. (1997). *Modelling Extremal Events for Insurance and Finance*. Springer, New York. <http://dx.doi.org/10.1007/978-3-642-33483-2>
12. Fraga Alves, M.I., Gomes, M.I., de Haan, L., Neves, C. (2009). Mixed moment estimator and location invariant alternatives. *Extremes*, 12, 149-185. <https://doi.org/10.1007/s10687-008-0073-3>
13. Fountoulakis, N., van Der Hoorn, P., Müller, T., Schepers, M. (2021). Clustering in a hyperbolic model of complex networks. *Electronic Journal of Probability*, 26, 1-132. <https://doi.org/10.1214/21-EJP583>
14. Gallotti, R., Barthelemy, M. (2015). Data from: The multilayer temporal network of public transport in Great Britain. *Scientific Data*, 2, 140056. <https://doi.org/10.5061/dryad.pc8m3>
15. Gemmetto, V., Barrat, A., Cattuto, C. (2014). Mitigation of infectious disease at school: targeted class closure vs school closure. *BMC Infectious Diseases*, 14, 695. <https://doi.org/10.1186/s12879-014-0695-9>
16. Ghoshal, G., Chi, L., Barabási, A.L. (2013). Uncovering the role of elementary processes in network evolution. *Scientific Reports*, 3, 2920. <https://doi.org/10.1038/srep02920>
17. Guimerá, R., Danon, L., Díazguilera, A., Giralt, F., Arenas, A. (2003). Selfsimilar community structure in a network of human interactions. *Physical Review E*, 68, 065103. <https://doi.org/10.1103/PhysRevE.68.065103>
18. Hill, B.M. (1975). A simple general approach to inference about the tail of a distribution. *Ann. Statist.*, 3, 1163-1174. <http://www.jstor.org/stable/2958370>
19. van der Hofstad, R. (2017). *Random Graphs and Complex Networks*. Vol. 1, Cambridge University Press.
20. Michielan, R., Litvak, N., Stegehuis, C. (2022). Detecting hyperbolic geometry in networks: why triangles are not enough. *Phys. Rev. E*, 106(5), 054303. <https://doi.org/10.1103/PhysRevE.106.054303>
21. Markovich, N.M. (2007). *Nonparametric Analysis of Univariate Heavy-Tailed data: Research and Practice*. Chichester, West Sussex: Wiley.
22. Markovich, N.M., Vaičiulis, M. (2024). Investigation of triangle counts in graphs evolved by uniform clustering attachment. *arXiv: 2401.11548v1*, 1-16.
23. Norros, I., Reittu, H. (2006). On a conditionally poissonian graph process. *Adv. Appl. Prob. (SGSA)*, 38, 59-75. DOI: 10.1239/aap/1143936140
24. Olive, X., Strohmeier, M., Lübbe, J. (2022). Crowdsourced air traffic data from The OpenSky Network. <https://zenodo.org/records/5815448>
25. Poursafaei, F., Huang, S., Pelrine, K., Rabbany, R. (2022). Towards better evaluation for dynamic link prediction. *Advances in Neural Information Processing Systems*, 35, 32928-32941.
26. Stehlé, J., Voirin, N., Barrat, A., Cattuto, C., Isella, L., Pinton, J.F., Quaghiotto, M., Van den Broeck, W., Régis, C., Lina, B., Vanhems, P. (2011). High-Resolution Measurements of Face-to-Face Contact Patterns in a Primary School. *PLoS ONE*, 6(8), e23176. <https://doi.org/10.1371/journal.pone.0023176>
27. Strohmeier, M., Olive, X., Lübbe, J., Schäfer, M., Lenders, V. (2021). Crowdsourced air traffic data from the OpenSky network 2019-2020. *Earth System Science Data Discussions*, 13(2), 357-366. <https://doi.org/10.5194/essd-13-357-2021>
28. Wan, P., Wang, T., Davis, R. A., Resnick, S.I. (2020). Are extreme value estimation methods useful for network data? *Extremes*, 23, 171-195. <https://doi.org/10.1007/s10687-019-00359-x>

Acknowledgements N. Markovich and M. Ryzhov were supported by the Russian Science Foundation (grant No. 24-21-00183).